



# Hourly River Flow Forecasting: Application of Emotional Neural Network Versus Multiple Machine Learning Paradigms

Zaher Mundher Yaseen<sup>1</sup> · Sujay Raghavendra Naganna<sup>2</sup> · Zulfaqar Sa'adi<sup>3</sup> · Pijush Samui<sup>4</sup> · Mohammad Ali Ghorbani<sup>5,6</sup> · Sinan Q. Salih<sup>7,8</sup> · Shamsuddin Shahid<sup>9</sup>

Received: 22 July 2019 / Accepted: 1 January 2020/  
Published online: 27 January 2020  
© Springer Nature B.V. 2020

## Abstract

Monitoring hourly river flows is indispensable for flood forecasting and disaster risk management. The objective of the present study is to develop a suite of hourly river flow forecasting models for the Albert river, located in Queensland, Australia using various machine learning (ML) based models including a relatively new and novel artificial intelligent modeling technique known as emotional neural network (ENN). Hourly river flow data for the period 2011–2014 is employed for the development and evaluation of the predictive models. The performance of the ENN model in forecasting hourly stage river flow is compared with other well-established ML-based models using a number of statistical metrics and graphical evaluation methods. The ENN showed an outstanding performance in terms of their forecasting accuracies, in comparison with other ML models. In general, the results clearly advocate the ENN as a promising artificial intelligence technique for accurate forecasting of hourly river flow in the form of real-time.

---

✉ Sinan Q. Salih  
sinanq.salih@duytan.edu.vn

Zaher Mundher Yaseen  
yaseen@tdtu.edu.vn

Sujay Raghavendra Naganna  
sujay.civil@sode-edu.in

Zulfaqar Sa'adi  
zulfaqar@utm.my

Pijush Samui  
pijushsamui@gmail.com

Mohammad Ali Ghorbani  
ghorbani@tabrizu.ac.ir

Shamsuddin Shahid  
sshahid@utm.my

Extended author information available on the last page of the article

**Keywords** Albert river · Emotional neural network · Machine learning · River flow · Time series forecasting

## 1 Introduction

Innovative technological advances for short-term forecasting of river flow is very much essential for mitigation and management of high intensity floods triggered due to unprecedented weather hazards. The land use changes significantly affect the runoff volumes as well as its time distributions (Sun et al. 2017). Recently, there has been an increase in the overall imperviousness due to rapid infrastructural developments in urban watersheds along with the transformations of river morphology and drainage systems causing relatively rapid storm water runoff (Muñoz et al. 2018). A timely update of rainfall contributions to river flow is made available routinely through river flow-gauging program which serves for planning and management of river flow. The benefits of long-term to short-term river flow forecasting include, the reservoir water management, erosion and sedimentation estimation, environmental flow assessment, planning of safe recreation programs, flood defence scheme design and warnings systems that accommodate disaster management authorities to manage and mitigate them at their early-onset (Hester et al. 2006). Additionally, the forecasting of peak river flows for desired return period has a prominent role in the hydraulic design of engineering structures. Therefore, new forecast models, particularly at very short-term (i.e., near real-time horizons) are immensely attractive for future decision-makers, including water resource management experts, flood forecasters, hydrologists, environmental monitoring and management experts (Yaseen et al. 2018b).

In published literature, there exist several researches that aim to address river flow and flood forecasting problems using process-oriented, stochastic, deterministic and more recently, machine learning based approaches (Zhou et al. 2019). In the last decade, hydrological time series forecasting based on ML approaches that aim to automate the analytical model building through data analysis has progressed in a tremendous way due to the availability of quality checked historical data records from a wide range of scientific and technological agencies (Fahimi et al. 2017). The river flow forecast models based on ML techniques can provide significant advantages over empirical and process-based models in terms of their robustness, level of accuracy, handling multi-dimensional data and the regularization's imposed on the model to avoid overfitting (Shortridge et al. 2016). The degree of uncertainty in process-oriented model outputs might also be higher because of a hurdle of model parameterization and explicitly stated assumptions (Chen et al. 2018). During the previous decades, considerable interest appears to be focused on the application of Artificial Neural Network (ANN) models of 15-min flow forecasts up to 6-h lead times (Dawson and Wilby 1998). Hourly flood forecasts of higher lead times (5-h) from ANNs were less accurate than 1-h forecasts owing to the basin characteristics and variations in the intensity of each flooding event. Several neural network variants evolved and for considerable period of time they were the only ones on board to provide accurate flood forecasts over all the lead times compared to other conceptual and linear stochastic models (Toth and Brath 2007). A detailed synthesis of literature related to river flow forecasting based on several ML models (published between the years 2000 to 2018) outlined in (Maier et al. 2010) and (Yaseen et al. 2018c) delivers insights on various kinds of techniques used, their advantages and, a comparative evaluation of individual model performances.

Hourly variations of river flow recorded from automated weather stations, that form the subject of this study, are very important as they can characterize hydrographs and flow duration

curves, without having to interpret or estimate peaks (Hailegeorgis and Alfredsen 2017). The inflection point differentiating the storm recession from base flow can easily be identified via hourly estimates of river flow. Additional statistics can also be computed from hourly river flow values, such as flood peaks, low flows, and their temporal variability while calibrating the flow hydrograph. Short-range river flow forecast (i.e., on an hourly basis) is hence, imperative for prediction of flood magnitude and its duration. It also helps in determination of river flow on time scales from days to years and thus, decision making for water resources management. Using conceptual rainfall-runoff models, (Bennett et al. 2016), generated hourly hydrological simulations from simple disaggregation of daily rainfalls records to hourly data and then verified against hourly river flow data. However, the approach is not viable for catchments that are smaller and more prone to rapid river flow responses. In tandem with terrain information, (Merkuryeva et al. 2015) processed river water level time series with trend extraction to predict the hourly river water levels by means of a symbolic regression-based forecasting model. It's worth noting that this approach requires heterogeneous data from both space and ground-based information sources. The ANN, Adaptive Neuro-fuzzy Inference System (ANFIS), Wavelet neural network (WNN) and, Wavelet ANFIS models were developed and applied by (Badrzadeh et al. 2015) for multiple hour lead-time flood forecasting at Casino station on Richmond River, Australia using hourly rainfall and runoff data. It's worth mentioning that neither ANN nor ANFIS models provided reliable simulations of flood events. Li et al. (2017) developed an extended version of Error Reduction and Representation In Stages (ERRIS) model to forecast river flow at hourly time steps by quantifying model uncertainties that reduce forecast errors. This model, however, showed poor performance in the bias-correction with respect to the catchments having shorter series of data records. In the light of the reported literature, hourly river flow forecasting is an interesting topic to be studied comprehensively and the exploration of newly developed ML models is always the passionate of the hydrology researchers to provide and accurate and reliable forecasting modeling strategy.

Although several ML models have been applied for modeling river flow simulation, the interest of exploring more reliable and robust predictive models is still ongoing research motivation. Especially, for solving some associated problem in the existed models or discovering new models' merits. Brian emotional learning is a recent discovered modeling strategy that is based on anatomical computation (Lotfi and Akbarzadeh-T 2014). The main merit of the ENN model is, there are two emotional responses during its learning including the anxiety and confidence. During the learning process, if the learning is momentous, then the confidence level is increased while the anxiety level is decreased (Lotfi and Akbarzadeh-T 2013). In addition, there are two additional emotional weights for the learning process which are not existed in the traditional ML models. The feasibility of the ENN model has been explored in diverse applications of water resources engineering (Sharghi et al. 2018, 2019; Nourani et al. 2019). However, for hourly scale river flow yet to be explored and investigated.

Considering the need for the hourly forecasts of river flow especially from a practical point of view, such as to provide near real-time forecasts of flood risk, the objective of the present research is to develop models for forecasting one-hour ahead hourly river flow using relatively a less explored ML tool known as Emotional Neural Network. To validate the utility of ENN compared to competing ML models, several well-established ML models were employed for validation including the Relevance Vector Machine (RVM), Minimax Probability Machine Regression (MPMR) and the Multivariate Adaptive Regression Splines (MARS). To the best of the authors' knowledge, there exist no study to assess the competence of different ML models introduced in this study for short-range river flow forecasting. Statistically significant

concurrent and correlated lagged data sets are used as the potential model inputs. The performance of the ML models in forecasting hourly river flow is comparatively evaluated using robust statistical score metrics and visual performance indicators.

## 2 Theoretical Overview

### 2.1 Emotional Neural Networks

This research paper explores the application of Emotional Neural Networks (ENN) to model hourly river flow for the first time, sighting its suitability in some previous studies, yet in different contexts, related to hydrological modeling (Nourani 2017; Sharghi et al. 2018). ENN is popularly used as forecasting tool in different fields due to its simplicity and quick training time. This back propagation (BP) learning algorithm was introduced by (Rumelhart et al. 1986) utilizing generalized delta rules for training a layered neural network. Khashman (2008) modified BP algorithm with the addition of two emotional coefficients to construct the emotional back propagation model. ENN model is thus an improved version of a conventional ANN model that incorporates an emotional system emitting artificial hormones that modulate the operation of each neuron in a feedback loop. Its basic structure consists of three layers: the input layer followed by a hidden layer and lastly the output layer, with  $i$ ,  $h$  and  $j$  neurons in their respective layers.

The data pre-processing and flow structure within the neural network from input layer to the output layer takes place in following phases. The neurons present in the input layer are non-processing and act as a carrier to pass the data, since its value and the output of each input-layer neuron is defined as follows:

$$YI_i = XI_i \quad (1)$$

where,  $XI_i$  and  $YI_i$  are the input and output values of neuron  $i$  in the input layer. The hidden neurons of ENN are represented as the processing neurons in the network where a sigmoidal function is usually used to activate each neuron for input feature extraction and subsequent modeling. Equation (2) gives the output of every hidden-layer neuron; which is usually a single layer however, this process will iterate even if there are more layers.

$$YH_h = \frac{1}{1 + \exp(-XH_h)} \quad (2)$$

where,  $XH_h$  and  $YH_h$  are respectively, the input and output values of neurons in the  $h$  hidden layer.

In order to obtain the input  $XH_h$  to a hidden layer neuron, the following equation is used.

$$XH_h = \sum_{i=1}^r W_{hi} \cdot YI_i \cdot W_{hb} \cdot X_b + W_{hm} \cdot X_m \quad (3)$$

where,  $W_{hi}$  is the weight provided by the hidden neuron  $h$  to the hidden layer  $i$  and  $YI_i$  is the output of the input neuron  $i$  and  $r$  is the maximum input-layer neurons.  $W_{hb}$  is the weight by hidden neuron  $h$  to the hidden layer bias neuron  $b$  and  $X_b$  is the input value to the bias neuron usually set to 1  $X_b=1$ .  $W_{hm}$  is the weight given by hidden neuron  $h$  to the hidden layer emotional neuron  $m$  and  $X_m$  is input value to the emotional neuron representing the global input pattern

average value  $Y_{PAT}$ . The applied transfer functions for ENN model were Tansing and Logsig with radial basis function kernel function.

## 2.2 Multivariate Adaptive Regression Splines

Multivariate adaptive regression splines (MARS) model introduced by (Friedman 1991) was also employed for hourly river flow prediction. MARS involves multivariate data to analyse the contributions from different predictors where interactive effects from explanatory data are used to forecast a target variable. It selects a regressor to implement with automatic smoothing (Krzyścin 2003) where inputs are split into subgroups and knots, located between different inputs and an interval to separate the subgroup (Friedman 1991; Sephton 2001). The MARS approach ensures adequate data in a subgroup, to avoid over-fitting by using shortest distance between neighbouring knots. Basis functions,  $BF_{(x)}$  are determined and projected on a target vector (Sharda et al. 2008). If  $X$  is the vector  $(x_1, x_2, \dots, x_N)$ , then:

$$Y = f(x) + \xi \quad (4)$$

where,  $N$  is the number of training datum points, and  $x_i$  is the distribution of error (Yaseen et al. 2018a). MARS model approximates the function  $f_{(x)}$  by applying basis functions  $BF_{(x)}$  having piece-wise function:  $\max(0, x-c)$ . The  $c$  represents the position of a knot, and  $\max_{(c)}$  indicates the positive part of  $(.)$ , otherwise it is zero, and is concordant with the following equation.

$$\max(0, x-c) = \begin{cases} x-c & \text{if } c \geq t \\ 0 & \text{otherwise} \end{cases} \quad (5)$$

If  $(X)$  is constructed as a linear combination of  $BF(x)$ .

$$f(x) = \beta_0 + \sum_{n=1}^{n=N} \beta_n BF(x) \quad (6)$$

where  $\beta$  is a constant estimated using least-squares and  $f(X)$  is a forward-backward stepwise method to identify the knots (Krzyścin 2003).

After the forward phase, an overlay elaborate model could result in, so a backward phase must be applied utilizing the Generalized Cross Validation (GCV). GCV estimates the mean square error (MSE) via the following equation (Zhang and Goh 2014).

$$GCV = \frac{MSE}{\left(1 - \frac{enp}{N}\right)^2} \quad (7)$$

where,  $enp$  is the effective number of parameters,  $enp = k + c(k-1)/2$ ;  $k$  is the number of basis functions in MARS model “equal to 10 in this study” (incl. Intercept term);  $c$  is a penalty (about 2 or 3);  $(k - 1)/2$  is the number of hinge-function knots, which penalize the addition of knots.

## 2.3 Minimax Probability Machine Regression

MPMR model utilizes a linear discriminant and convex optimization, which are indeed an improved version of support vector machines (Strohmann and Grudic 2003). In MPMR, the

data are analysed by shifting all regression data (+ε) along a dependent variable axis and the objective variable is analysed by shifting all regression data (−ε) along the dependent axis. The boundary is a regression surface where a model is trained to identify the bounds of probabilities for misclassifying a point without any assumption (Bertsimas and Sethuraman 2000). Consider a learning space (D-dimensional) from unknown regression function  $f : \mathfrak{R}^D \mathfrak{R}$  an MPMR model is written as (Strohmann and Grudic 2003):

$$y = f(X) + \rho \tag{8}$$

where,  $X \in \mathfrak{R}^D$  is an input vector within a bounded distribution  $\Omega$ ,  $Y \mathfrak{R}$  is an output vector and variance ( $\rho$ ) =  $\sigma^2 \mathfrak{R}$ . MPMR aims to create an approximation  $\hat{f}$  where for  $x_i$  generated from  $\Omega$ ,  $\hat{y}$  is given by (Strohmann and Grudic 2003):

$$\hat{y} = \hat{f}(x) \tag{9}$$

The model estimates the bounds on minimum probability  $\psi$  that  $\hat{f}$  within  $\varepsilon$  of  $Y$  (Lanckriet et al. 2003):

$$\psi = \inf Pr \{ |\hat{y} - y| \leq \varepsilon \} \tag{10}$$

Equation (10) estimates a true regression by a bound on minimax probability and deduces  $\psi$  within of a true function. A final MPMR model based on kernel formulation is therefore written as (Strohmann and Grudic 2003):

$$\hat{y} = \hat{f}(x) = \sum_{i=1}^N \beta_i K(x_i, x_j) + \rho \tag{11}$$

where,  $K_{i,j} = \varphi(x_i, x_j)$  is the kernel function satisfying mercer conditions and vector  $x_i$  is from the learned data and  $\beta_i$  and  $\rho$  are the output parameters. The MPMR model was developed with radial basis function width equal to 0.5 and error insensitive equal to 0.004.

### 2.4 Relevance Vector Machine

As a final benchmark model, Relevance Vector Machine (RVM) was applied. RVM proposed by (Tipping 2001) is an extension of support vector machine within a Bayesian context. A brief description of RVM framework is presented here but for greater details, the readers should refer (Tipping 2001). In this article, the RVM algorithm is considered a predictor for a set of inputs ( $x$ ) according to:

$$E = f(x, w) + \varepsilon_n \tag{12}$$

In Eq. (12), the error term  $\varepsilon_n = N(0, \sigma^2)$  is a zero mean gaussian process and  $w = (w_0, \dots, w_n)^T$  are the vectors of weights. The likelihood of the complete data can be represented as follows:

$$p\left(\frac{E}{w}, \sigma^2\right) = (2\pi\sigma^2)^{-N/2} \cdot \exp\left\{-\frac{1}{2\sigma^2} \|E - \Phi w\|^2\right\} \tag{13}$$

where,  $\Phi(X_i) = [1, K(x_i, x_1), K(x_i, x_2), \dots, K(x_i, x_N)]^T$ . Without imposing hyper-parameters on the weights,  $w$ , the maximum likelihood can suffer from over fitting. Following (Tipping 2001), a constraint,  $w$  is imposed by a complexity penalty to the likelihood or error function

and an explicit zero mean gaussian prior probability distribution over the weights,  $w$ , with a diagonal covariance,  $\alpha$  is adopted:

$$p(w/\alpha) = \prod_{i=0}^N N(w_i/0, \alpha_i^{-1}) \quad (14)$$

where,  $\alpha$  = vector of  $N + 1$  hyper-parameters. The Bayes rule is applied to calculate the posterior over all unknowns given the defined non-informative prior distribution that follows:

$$p(w, \alpha, \sigma^2/E) = \frac{p(E/w, \alpha, \sigma^2).p(w, \alpha, \sigma^2)}{\int p(E/w, \alpha, \sigma^2).p(w, \alpha, \sigma^2)dw d\alpha d\sigma^2} \quad (15)$$

It is important to note that the analytic solution is inexorable, so a decomposition of the posterior according to  $p(w, \alpha, \sigma^2/E) = (E/w, \alpha, \sigma^2)$ .  $p(\alpha, \sigma^2/E)$  is used where the posterior distribution over the weights is written as:

$$\begin{aligned} p(w/E, \alpha, \sigma^2) &= \frac{p(E/w, \sigma^2).p(w/\alpha)}{p(E/\alpha, \sigma^2)} \\ &= (2\pi)^{-(N+1)/2} \Sigma^{-1/2} \exp\left\{-\frac{1}{2}(w-\mu)^T \Sigma^{-1}(w-\mu)\right\} \end{aligned} \quad (16)$$

The posterior covariance and mean can be listed as:

$$\begin{aligned} \Sigma &= (\sigma^{-2} \Phi^T \Phi + A)^{-1} \\ \mu &= \sigma^{-2} \Sigma \Phi^T E \end{aligned} \quad (17)$$

with  $A = \text{diag}(\alpha_0, \alpha_1, \dots, \alpha_N)$ . In the learning process, a search for hyper-parameters posterior is done by maximization of  $p(\alpha, \sigma^2/E) \propto p(\frac{E}{\alpha}, \sigma^2)p(\alpha^2)$  with respect to  $\alpha$  and  $\sigma^2$ . For a uniform hyper-prior over  $\alpha$  and  $\sigma^2$ , the term  $p(\frac{E}{\alpha}, \sigma^2)$  is minimized as:

$$\begin{aligned} \rho(E/a, \sigma^2) &= \int \rho(E/w, \sigma^2) \rho(w/a) dw \\ &= \left( (2\pi)^{-\frac{N}{2}} / \sqrt{|\sigma^2 + \Phi A^{-1} \Phi^T|} \times \exp\left\{-\frac{1}{2} E^T (\sigma^2 + \Phi A^{-1} \Phi^T)^{-1} E\right\} \right) \end{aligned} \quad (18)$$

The maximization of the quantity  $\rho(E/a, \sigma^2)$  is known as the type II maximum likelihood method, also the evidence of hyper-parameter (Barto 1985). To attain an optimal RVM mode, an iterative formula is used to determine the hyper-parameters (Tipping 2001). RVM model was conducted with kernel radial basis function with width equal to 0.3.

### 3 Study Area and Model Data Set

The Albert River is a perennial river located in the South East region of Queensland, Australia with its headwaters in Lamington National Park McPherson Ranges (see Fig. 1). Its catchment lies within the Gold Coast, Logan City and Scenic Rim Region council's boundaries and covers an area of 782 km<sup>2</sup>. The Albert River is a large tributary of the Logan River which has a confluence with the Logan River some 25 km downstream of the boundary. The river starts near Hillview at an elevation of 184 m and ends at an elevation of 3.47 m merging with the Logan River near Beenleigh and the Logan then flows to southern Moreton Bay. It is a long

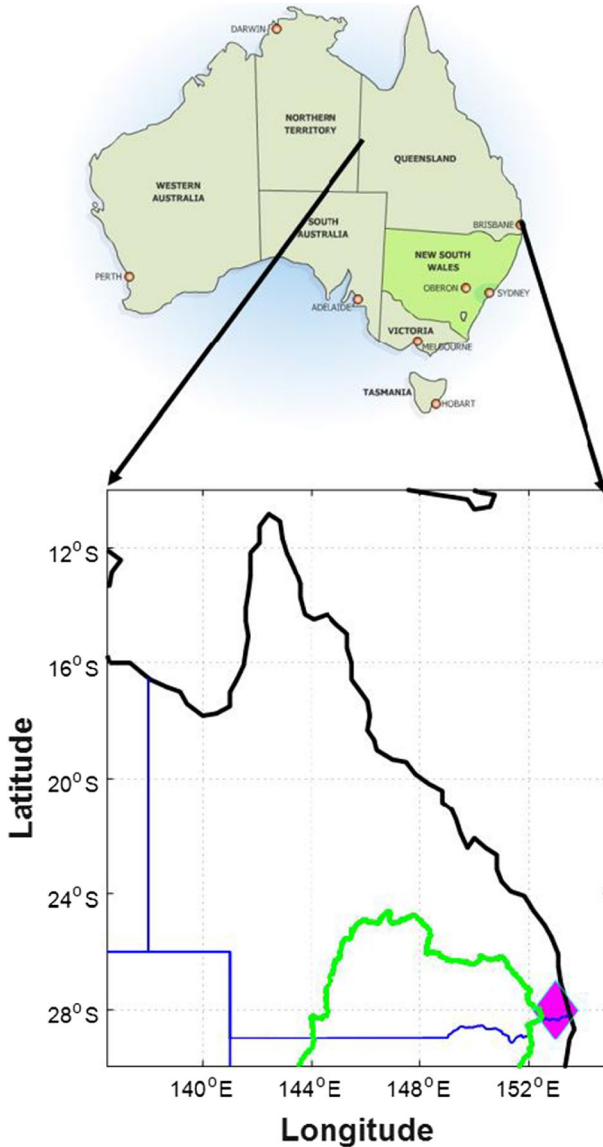


**Fig. 1** The location of Albert river in the south region of Queensland, Australia

narrow catchment in which the major streams flow from south to north dropping around 181 m over its 102 km length. The major soil type in the catchment is loam with varying texture profiles. Friable earths and cracking clays are also found in the area. The Albert catchment experiences very high average rainfall in the headwaters, with approximately 1600 mm per year at O'Reilly rain gauge station. This very high rainfall combined with good recharge of groundwater associated with the predominant basalt results in near-permanent flow. There are occasional landslips, which erode large areas of bank and increase sedimentation further downstream. It is estimated that during the 2008 flood event, approximately 70% of sediment in the Logan Estuary was derived from these Lamington Group rocks. The rest of the



catchment experiences high to moderate average rainfall, with the slopes and coastal areas receive more rainfall than the low-lying mid reaches. These different rainfall levels combine to make up the rainfall of the Albert Catchment.

In this paper, a relatively lengthy dataset spanning hourly river flow values, from 1/01/2009 (5:00:00 AM) to 31/12/2014/ (00:00:00 AM) were used to develop ENN and MARS models. This comprises of 52,555 values that partitioned manually into training (60% “31,533 values”), validation (20% “10,511 values”) and testing (20% “10,511 values”) subsets. This dataset is significantly long to provide the input features of the predictive model. In accordance with PACF plot, a total of 3 statistically significant lagged inputs were used to model 1-h lead time river flow values.

#### 4 Model Development and Performance Evaluation Measures

The performance of developed models depends on the dataset and design parameters. The design parameters are determined by trial and error approach. The normalized dataset (between 0 and 1) was employed for model development. The normalization process has been done to avoid the high magnitude variance in the actual data and simulate the data within an acceptable range (0–1) for the software modeling environment (Khosravi et al. 2018). The forecasting accuracy of the proposed predictive models were evaluated using various statistical formulations including Correlation coefficient ( $r$ ), Normalized root mean square error ( $RMSE$ ), Percent Bias (PBIAS), Nash-Sutcliffe Efficiency ( $NSE$ ), Modified Index of Agreement ( $md$ ), Persistence Index ( $cp$ ), Relative index of agreement ( $rd$ ), Kling-Gupta efficiency ( $KGE$ ). Mathematically, the statistical formulations are expressed as follows:

$$r = \frac{\sum_{i=1}^N (X_o - \bar{X}_o) (X_f - \bar{X}_f)}{\sqrt{\sum_{i=1}^N (X_o - \bar{X}_o)^2} \sqrt{\sum_{i=1}^N (X_f - \bar{X}_f)^2}} \quad (19)$$

$$RMSE = \sqrt{\frac{1}{N} \sum_{i=1}^N (X_f - X_o)^2} \quad (20)$$

$$MAE = \frac{1}{N} \sum_{i=1}^N |X_f - X_o|$$

$$PBIAS = \frac{\sum_{i=1}^N (X_o - X_f)}{\sum_{i=1}^N X_f} \quad (21)$$

$$NSE = 1 - \left[ \frac{\sum_{i=1}^N (X_o - X_o)^2}{\sum_{i=1}^N (X_o - \bar{X}_o)^2} \right] \quad (22)$$

$$md = 1 - \frac{\sum_{i=1}^N (X_o - X_f)^j}{\sum_{i=1}^N (|X_f - \bar{X}_o| + |X_o - \bar{X}_o|)^j} \quad (23)$$

$$rd = 1 - \frac{\sum_{i=1}^N \left(\frac{X_o - X_f}{X_o}\right)^2}{\sum_{i=1}^N \left(\frac{(|X_f - \bar{X}_o| + |X_o - \bar{X}_o|)}{\bar{X}_o}\right)^2} \tag{24}$$

$$KGE = 1 - \sqrt{(r-1)^2 + (\alpha-1)^2 + (\beta-1)^2} \tag{25}$$

where  $X_o$  and  $X_f$  are the actual and forecasted river flow,  $\bar{X}_o$  and  $\bar{X}_f$  are the mean values,  $r$  is the linear correlation between actual and forecasted,  $\alpha$  is the variability  $\alpha = \sigma_f/\sigma_o$ ,  $\beta$  is the bias term  $\beta = \mu_f/\mu_o$ .  $J$  is the exponent term.  $N$  is the number of observations. The physical explanation of the computed statistical formulations can be found in the following researches (Dawson et al. 2007; Chadalawada and Babovic 2019).

### 5 Results and Discussion

The input attributes of the models were constructed based on the partial auto-correlation function (PACF). PACF provides information about the correlation between two separate points on the time-series at different time lags and provides information about the repeating patterns in the time-series. PACF value ranges between 1 and  $-1$ ; the value near to 1 indicates near perfect correlation and the value near to  $-1$  indicates complete anti-correlation. In this study, the PACF values equal to or more than 0.5 were considered for the selection of time-lag pattern. Figure 2 illustrates the PACF values for different time lags up to 12 h. It could be observed that the PACF values for the time-lags (t-1), (t-2) and (t-3) were more or less equal to 0.5 and therefore, Q(t-1), Q(t-2) and Q(t-3) were selected as inputs for forecasting one-hour ahead river flow using the predictive models.

The performance of all the ML models in forecasting hourly river flow during model training and testing phases were evaluated using several statistical indices including  $r$ ,  $R^2$ ,  $RMSE$ ,

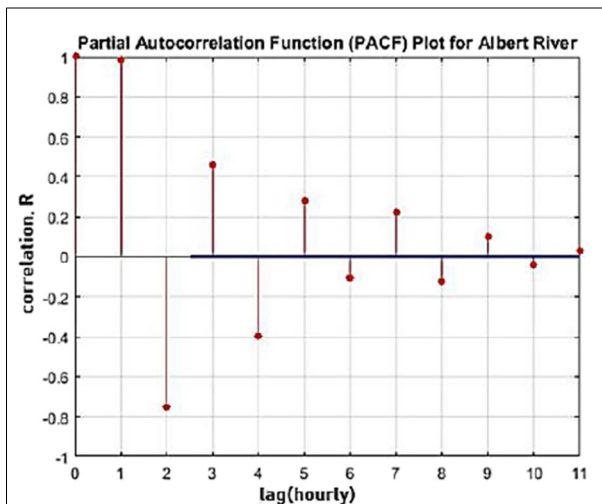


Fig. 2 The partial auto-correlation function (PACF) of historical river flow data of Albert River

**Table 1** The models performance based on correlation coefficient ( $r$ ), coefficient of determination ( $R^2$ ), Root mean square errors (RMSE), Mean Absolute Error (MAE), Nash-Sutcliffe Efficiency (NSE), Modified Index of Agreement ( $md$ ), relative Index of Agreement ( $rd$ ) and Kling-Gupta efficiency (KGE) for hourly river flow simulation over the training and testing phases

Model	$r$	$R^2$	RMSE	PBIAS	MAE	NSE	$md$	$rd$	KGE
Train									
ENN	0.9976	0.9953	49.91	0	5.32	1	0.98	1.00	1.00
MARS	0.9980	0.9962	45.10	0	4.39	1	0.99	1.00	1.00
MPMR	0.9980	0.9962	45.10	0	4.39	1	0.99	1.00	1.00
RVM	0.9347	0.8737	258.86	-51	213.46	0.8	0.45	0.97	0.46
Test									
ENN	0.9940	0.9881	25.07	-8.1	3.13	0.99	0.94	1.00	0.92
MARS	0.9931	0.9863	27.23	-1.4	4.13	0.99	0.97	1.00	0.97
MPMR	0.9521	0.9066	75.49	-58.8	38.54	0.88	0.48	0.99	0.41
RVM	0.9731	0.9471	290.85	-92.8	287.46	-0.59	0.12	0.69	0.07

*PBIAS*, *MAE*, *NSE*, *md*, *rd*, and *KGE*. Table 1 shows that ENN, MARS and MPMR performed well in terms of  $r$  and  $R^2$  during training phase. The results showed high degree of linearity between the simulated and the observed data with high predictive ability for all models. A positive linear relationship and higher coefficient value greater than 0.95 was obtained during training phase. Whereas, over the testing phase the  $r$  values were very satisfactory and indicated less error variance for each model. However, ENN and MARS models were observed to give the lowest level of scatter appearance (Fig. 3). Although  $r$  and  $R^2$  have been widely used for model evaluation, it is oversensitive to high extreme values and insensitive to additive and proportional differences between model predictions and observed data (Legates and Jr 1999; Moriasi et al. 2007).

*MAE* is considered in this study as its evaluation is less sensitive to extreme values in the forecast data than the *RMSE* (Fox 1981). ENN (5.32, 25.07) and MARS (4.39, 27.23) demonstrate the lowest deviation from the observed values compared to MPMR (4.39, 75.49) and RVM (213.46, 287.46) for the training and testing phase. Studies reported *NSE* is a normalized statistic that determines the relative magnitude of the residual variance compared to the measured data variance (Nash and Sutcliffe 1970). *NSE* values were found to be ideal ( $NSE = 1$ ) for the training phase of ENN, MARS and MPMR models while for RVM model ( $NSE = 0.8$ ). According to the guidelines of hydrological model performance evaluation proposed by (Moriasi et al. 2007), the performance of a hydrological model is very good if *NSE* is more than 0.75. Therefore, it can be remarked that all the models performed very good during the training phase. However, among these models, ENN and MARS models ( $NSE = 0.99$ ) that is indicated better performance against MPMR ( $NSE = 0.88$ ) and RVM ( $NSE = -0.59$ ) over the testing phase. The modified index of agreement (*md*) developed by (Willmott 1981) as a standardized measure of the degree of model prediction error showed that ENN (0.98, 0.94) and MARS (0.99, 0.97) give the best model fit than MPMR (0.99, 0.48) and RVM (0.45, 0.12) for training and testing phases. Although *md* provides some improvement over  $R^2$ , it is still sensitive to extreme values due to the squared differences in the mean square error in the numerator (Legates and Jr 1999). In addition, the disadvantage of the results given by the previous  $R^2$  and *NSE* arises from the fact that the differences of observed and predicted river flow use the squared values. Consequently, large errors in time series can be overestimated whereas small values can be neglected. To reduce the effect of absolute differences during peak flows and to improve the effect of absolute low flow differences, *rd* was subsequently applied to measure the differences between the observed and simulated values as relative deviations (Chadalawada and Babovic 2019).

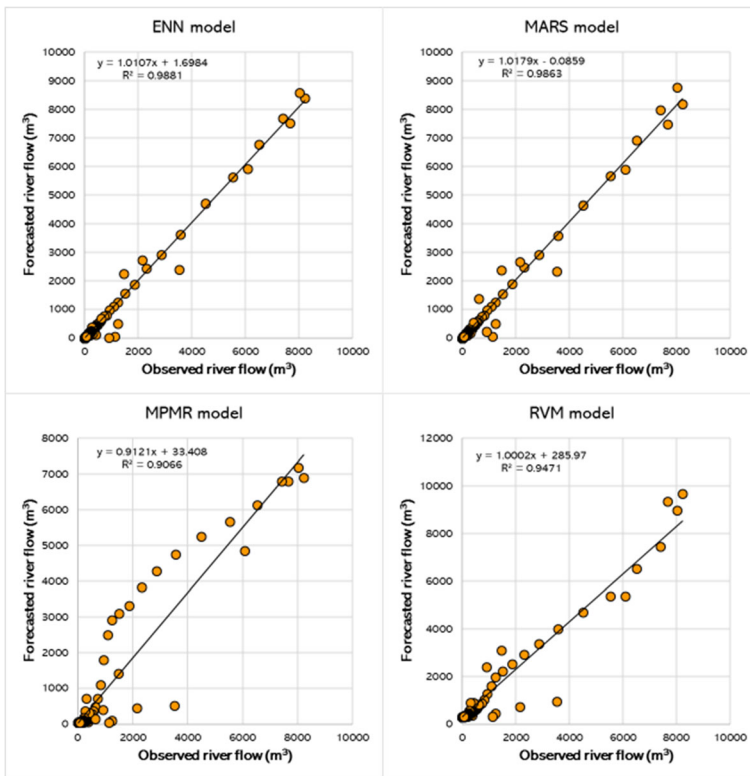


**Fig. 3** A scatter plot of hourly simulated and observed river flow during the testing period (Jan 2014 - Dec 2014) for ENN, MARS, MPMR and RVM models

A perfect match (1.00) was obtained under  $rd$  for ENN and MARS compared with MPMR (1.00, 0.99) and RVM (0.97, 0.69) for the training and testing phases.

In this study, a refine version of  $KGE$  proposed by (Gupta 2011), was used to provide a diagnostically interesting decomposition of the  $NSE$ , which facilitates the analysis of the relative importance of its different components (correlation, bias and variability) in the context of hydrological modelling (Gupta et al. 2009). ENN (1.00, 0.92) and MARS (1.00, 0.97) give the best result with  $KGE$  compare to MPMR (1.00, 0.41) and RVM (0.46, 0.07) for the training and testing phases.

Percent bias (PBIAS) measures the average tendency of the simulated data to be either higher or lower compared to the observed data. According to (Moriassi et al. 2007), the  $PBIAS < \pm 10$  indicates very good performance of river flow model. Based on this criterion, only ENN (0.0, -8.1) and MARS (0.0, -1.4) were found to perform very good during training and testing phases. However, there was observed a low degree of overestimation (negative value) for the testing phase of the forecast in capturing the extreme river flow. In terms of all these statistics, clearly ENN and MARS were found to perform much better compared to MPMR and RVM during training and testing phases. The performance of the ENN was found very close to MARS in terms of all statistics presented in Table 1.

The performance of the predictive models was also evaluated through visual inspection of graphical representations of the results. Scatter plots were useful to have better understanding of how well the models have estimated the observed data. The scatter plot over the testing

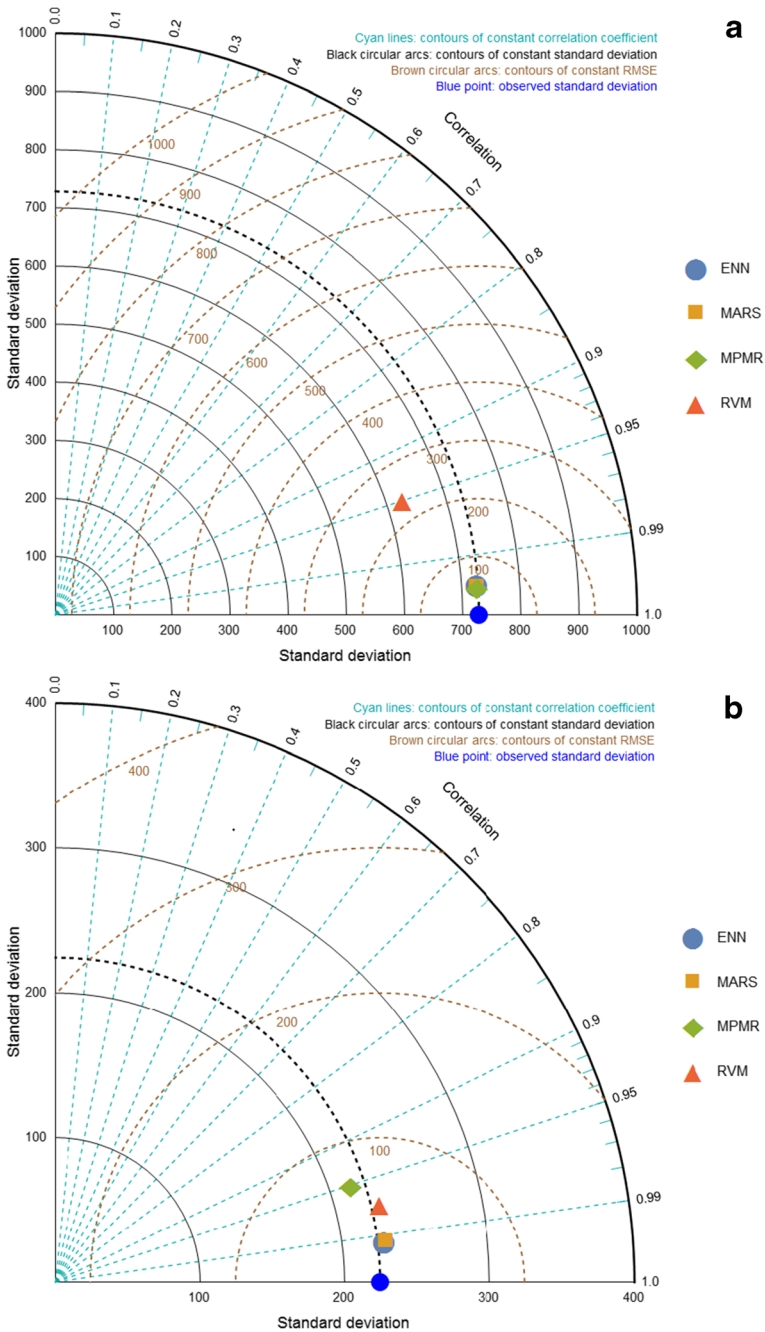


**Fig. 4** Taylor diagram of the hourly river flow at Albert River, (a) training, (b) testing phases of ENN, MARS, MPMR and RVM models, showing their efficiency compared to observed river flow

phase shows that almost all the points were aligned along the diagonal line of the plots for both ENN and MARS (Fig. 3). However, the magnitude of the coefficient of determination was

slightly better for the ENN model over the testing phase. ENN model was attained  $R^2 = 0.9881$ ; whereas, MARS model was attained  $R^2 = 0.9863$ . On the other hand, a large deviation, particularly in forecasting higher river flow was noticed for MPMR and RVM.

Taylor diagram was used to show how the predicted river flow by different models are in proximity of observed river flow in terms of correlation, standard deviation and *RMSE*. Figure 4 shows that ENN and MARS were in the closest proximity to observed river flow during model training and testing. Moriasi et al. (2007) stated that a very good hydrological model should have a *RMSE* less than 50% of the standard deviation (SD) of the data. Taylor diagram shows that the ratio of *RMSE* and SD for both ENN and MARS simulated river flow was much less than 0.5 during training and testing phases. However, compared to MARS, the ENN was found much closer to observed point during model testing phase. The ENN predicted river flow was found to have almost same standard deviation of observed river flow during training and testing phases.

All the models were capable to replicate the observed distribution of river flow during model training and testing phases. However, during models testing, the ENN and MARS were found to replicate the spread of data more accurately compared to MPMR and RVM. To summarize, it can be remarked that ENN and MARS were found to have higher capability to predict hourly river flow compared to MPMR and RVM. Between MPMR and RVM, the MPMR was found much better compared to RVM, which was found to perform worst during model testing in term of all statistics. The performance of ENN and MARS were found very close to each other in term of all statistics. However, visual inspection of scatter plots, Taylor diagrams and violin plots reveal marginally higher performance of ENN compared to MARS.

While this study has set a foundation to apply ENN for river flow forecasting over hourly scales, and the study strongly supports recent work that developed an hourly water monitoring index (Deo et al. 2018), further research on multiple lead times would also be useful. Such research would provide users of the model new information on how river flow and how it be predicted over longer-term horizons. While it is a useful subject, that sort of study was beyond the scope of the present work and can form a useful subject for further investigation in future where ENN model could be developed over hourly as well as other lead times. It is worth to mention, the application of the ML models in the stage of advancement and development. ML models are hyper-parameter models in which their modeling performance depend of on the modeling tuning (Chau 2019). However, ML models demonstrated an excellent performance in solving the stochastic problem in the hydrological engineering field.

## 6 Conclusions

In this study, a relatively less explored ML models, ENN was used for the forecasting of hourly river flow and its performance was compared with three recently developed ML models, namely MARS, MPMR and RVM which are considered competing models in the hydrological forecasting. The main aim of the current study was to develop a reliable intelligent model for hourly scale river flow forecasting and thus the application of ENN model for the first time in forecasting river flow. A case study of Albert River which is located in southeast Queensland, was examined. Flood is a challenging issue in the river basin and therefore, short-term river flow forecasting is an important task for water resource and flood risk management. The statistical assessment of the predictive models reveals superiority of the ENN and MARS models over the MPMR and RVM models. Both the ENN and the MARS models showed  $R^2$  and an *NSE* values near to unity and relatively low

errors during model testing, which indicate their excellent ability in forecasting hourly river flow. The scatter plots over the testing phase were evidenced the ability of both the ENN and MARS models to reproduce most of the values of the river flow including the extreme river flows with minimum error. However, the ENN model was found to perform marginally better than MARS when the model performance was assessed statistically. Similar to several other ML models, ENN model is associated with the hyper-parameter limitation and thus its internal parameters could be optimized using the advanced nature inspired optimization algorithms that can be investigated in future research. In addition, the capacity of the proposed ENN model can further studied through the investigation of different data division scenarios for the training and testing phases.

**Acknowledgements** The authors thank Associate Professor Ravinesh Deo for providing the river flow data and his constructive comments on establishing this research. In addition, we do acknowledge the valuable comments reported by the respected reviewers to enhance the manuscript presentation and readability. Further, our appreciation is extended to the editor-in-chief and the associated editor for handling our manuscript.

## Compliance with Ethical Standards

**Conflict of Interest** Authors declare no conflict of interest.

## References

- Badrzadeh H, Sarukkalige R, Jayawardena AW (2015) Hourly runoff forecasting for flood risk management: application of various computational intelligence models. *J Hydrol* 529:1633–1643. <https://doi.org/10.1016/j.jhydrol.2015.07.057>
- Barto AG (1985) Learning by statistical cooperation of self-interested neuron-like computing elements. *Hum Neurobiol* 4:229–256
- Bennett JC, Robertson DE, Ward PGD et al (2016) Calibrating hourly rainfall-runoff models with daily forcings for streamflow forecasting applications in meso-scale catchments. *Environ Model Softw* 76:20–36. <https://doi.org/10.1016/j.envsoft.2015.11.006>
- Bertsimas D, Sethuraman J (2000) Moment problems and Semidefinite optimization. *Int Ser Oper Res Manag Sci* 469–509
- Chadalawada J, Babovic V (2019) Flood forecasting based on an improved extreme learning machine model combined with the backtracking search optimization algorithm. *J Hydroinf* 21:13–31. <https://doi.org/10.2166/hydro.2017.078>
- Chau K (2019) Integration of advanced soft computing techniques in hydrological predictions. *Atmosphere (Basel)* 10:101. <https://doi.org/10.3390/atmos10020101>
- Chen L, Sun N, Zhou C et al (2018) Flood forecasting based on an improved extreme learning machine model combined with the backtracking search optimization algorithm. *Water* 10:1362. <https://doi.org/10.3390/w10101362>
- Dawson CW, Wilby R (1998) An artificial neural network approach to rainfall-runoff modelling. *Hydrol Sci J* 43: 47–66. <https://doi.org/10.1080/02626669809492102>
- Dawson CW, Abrahart RJ, See LM (2007) HydroTest: a web-based toolbox of evaluation metrics for the standardised assessment of hydrological forecasts. *Environ Model Softw* 22:1034–1052. <https://doi.org/10.1016/j.envsoft.2006.06.008>
- Deo RC, Byun H-R, Kim G-B, Adamowski JF (2018) A real-time hourly water index for flood risk monitoring: pilot studies in Brisbane, Australia, and Dobong observatory, South Korea. *Environ Monit Assess* 190:450. <https://doi.org/10.1007/s10661-018-6806-0>
- Fahimi F, Yaseen ZM, El-shafie A (2017) Application of soft computing based hybrid models in hydrological variables modeling: a comprehensive review. *Theor Appl Climatol* 128:875–903. <https://doi.org/10.1007/s00704-016-1735-8>
- Fox DG (1981) Judging air quality model performance: a summary of the AMS workshop on dispersion model performance, woods hole, Mass., 8–11 September 1980. *Bull Am Meteorol Soc* 62:599–609
- Friedman JH (1991) Multivariate adaptive regression splines. *Ann Stat* 19:1–67. <https://doi.org/10.1214/aos/1176347963>
- Gupta SK (2011) Fundamentals of hydrology. In: *Modern hydrology and sustainable water development*, pp 1–19

- Gupta HV, Kling H, Yilmaz KK, Martinez GF (2009) Decomposition of the mean squared error and NSE performance criteria: implications for improving hydrological modelling. *J Hydrol* 377:80–91. <https://doi.org/10.1016/j.jhydrol.2009.08.003>
- Hailegeorgis TT, Alfredsen K (2017) Regional statistical and precipitation–runoff Modelling for ecological applications: prediction of hourly Streamflow in regulated Rivers and Ungauged basins. In: *River Research and Applications*
- Hester G, Carsell K, Ford D (2006) Benefits of USGS streamgaging program—users and uses of USGS streamflow data. *Natl Hydrol Wam Council*:1–18
- Khashman A (2008) A modified backpropagation learning algorithm with added emotional coefficients. *IEEE Trans Neural Netw* 19:1896–1909. <https://doi.org/10.1109/TNN.2008.2002913>
- Khosravi K, Mao L, Kisi O et al (2018) Quantifying hourly suspended sediment load using data mining models: case study of a glacierized Andean catchment in Chile. *J Hydrol* 567:165–179. <https://doi.org/10.1016/j.jhydrol.2018.10.015>
- Krzyżściński JW (2003) Nonlinear (MARS) modeling of long-term variations of surface UV-B radiation as revealed from the analysis of Belsk, Poland data for the period 1976–2000. *Ann Geophys* 21:1887–1896. <https://doi.org/10.5194/angeo-21-1887-2003>
- Lanckriet GRG, El Ghaoui L, Bhattacharyya C, Jordan MI (2003) A robust minimax approach to classification. In: *Journal of Machine Learning Research*
- Legates DR, Jr GJM (1999) Evaluating the use of “goodness-of-fit” measures in hydrologic and hydroclimatic model validation. *Water Resour Res* 35:233–241
- Li M, Wang QJ, Robertson DE, Bennett JC (2017) Improved error modelling for streamflow forecasting at hourly time steps by splitting hydrographs into rising and falling limbs. *J Hydrol*. <https://doi.org/10.1016/j.jhydrol.2017.10.057>
- Lotfi E, Akbarzadeh-T MR (2013) Brain emotional learning-based pattern recognizer. *Cybern Syst*. <https://doi.org/10.1080/01969722.2013.789652>
- Lotfi E, Akbarzadeh-T MR (2014) Practical emotional neural networks. *Neural Netw* 59:61–72. <https://doi.org/10.1016/j.neunet.2014.06.012>
- Maier HR, Jain A, Dandy GC, Sudheer KP (2010) Methods used for the development of neural networks for the prediction of water resource variables in river systems: current status and future directions. *Environ Model Softw* 25:891–909. <https://doi.org/10.1016/j.envsoft.2010.02.003>
- Merkuryeva G, Merkuryev Y, Sokolov BV et al (2015) Advanced river flood monitoring, modelling and forecasting. *J Comput Sci* 10:77–85. <https://doi.org/10.1016/j.jocs.2014.10.004>
- Moriasi DN, Arnold JG, Van Liew MW et al (2007) Model evaluation guidelines for systematic quantification of accuracy in watershed simulations. *Trans ASABE* 50:885–900. <https://doi.org/10.13031/2013.23153>
- Muñoz LA, Olivera F, Giglio M, Berke P (2018) The impact of urbanization on the streamflows and the 100-year floodplain extent of the Sims bayou in Houston, Texas. *Int J River Basin Manag*. <https://doi.org/10.1080/15715124.2017.1372447>
- Nash JE, Sutcliffe JV (1970) River flow forecasting through conceptual models part I—a discussion of principles\*. *J Hydrol* 10:282–290. [https://doi.org/10.1016/0022-1694\(70\)90255-6](https://doi.org/10.1016/0022-1694(70)90255-6)
- Nourani V (2017) An emotional ANN (EANN) approach to modeling rainfall–runoff process. *J Hydrol* 544:267–277. <https://doi.org/10.1016/j.jhydrol.2016.11.033>
- Nourani V, Molajou A, Najafi H, Mehr AD (2019) Emotional ANN (EANN): a new generation of neural networks for hydrological modeling in IoT, Artificial Intelligence in IoT. Springer, pp 45–61
- Rumelhart DE, Hinton GE, Williams RJ (1986) Learning representations by back-propagating errors. *Nature* 323:533–536. <https://doi.org/10.1038/323533a0>
- Sephton P (2001) Forecasting recessions: can we do better on MARS? *Review* 83:39–49
- Sharda VN, Prasher SO, Patel RM et al (2008) Performance of multivariate adaptive regression splines (MARS) in predicting runoff in mid-Himalayan micro-watersheds with limited data. *Hydrol Sci J* 53:1165–1175. <https://doi.org/10.1623/hysj.53.6.1165>
- Sharghi E, Nourani V, Najafi H, Molajou A (2018) Emotional ANN (EANN) and wavelet-ANN (WANN) approaches for Markovian and seasonal based modeling of rainfall–runoff process. *Water Resour Manag* 32:3441–3456. <https://doi.org/10.1007/s11269-018-2000-y>
- Sharghi E, Nourani V, Molajou A, Najafi H (2019) Conjunction of emotional ANN (EANN) and wavelet transform for rainfall–runoff modeling. *J Hydroinf* 21:136–152. <https://doi.org/10.2166/hydro.2018.054>
- Shortridge JE, Guikema SD, Zaitchik BF (2016) Machine learning methods for empirical streamflow simulation: a comparison of model accuracy, interpretability, and uncertainty in seasonal watersheds. *Hydrol Earth Syst Sci* 20:2611–2628. <https://doi.org/10.5194/hess-20-2611-2016>
- Strohmann T, Grudic GZ (2003) A formulation for minimax probability machine regression. In: *Advances in Neural Information Processing Systems*. pp 785–792



- Sun Z, Lotz T, Chang N-B (2017) Assessing the long-term effects of land use changes on runoff patterns and food production in a large lake watershed with policy implications. *J Environ Manag* 204:92–101. <https://doi.org/10.1016/j.jenvman.2017.08.043>
- Tipping ME (2001) Sparse Bayesian learning and the relevance vector machine. *J Mach Learn Res* 1:211–244. <https://doi.org/10.1162/15324430152748236>
- Toth E, Braith A (2007) Multistep ahead streamflow forecasting: role of calibration data in conceptual and neural network modeling. *Water Resour Res* 43:1–11. <https://doi.org/10.1029/2006WR005383>
- Willmott CJ (1981) On the validation of models. *Phys Geogr* 2:184–194
- Yaseen ZM, Deo RC, Hilal A et al (2018a) Predicting compressive strength of lightweight foamed concrete using extreme learning machine model. *Adv Eng Softw* 115:112–125. <https://doi.org/10.1016/j.advengsoft.2017.09.004>
- Yaseen ZM, Fu M, Wang C, Mohtar WHMW, Deo RC, el-shafie A (2018b) Application of the hybrid artificial neural network coupled with rolling mechanism and Grey model algorithms for Streamflow forecasting over multiple time horizons. *Water Resour Manag* 32:1883–1899. <https://doi.org/10.1007/s11269-018-1909-5>
- Yaseen ZM, Sulaiman SO, Deo RC, Chau K-W (2018c) An enhanced extreme learning machine model for river flow forecasting: state-of-the-art, practical applications in water resource engineering area and future research direction. *J Hydrol* 569:387–408. <https://doi.org/10.1016/j.jhydrol.2018.11.069>
- Zhang W, Goh ATC (2014) Multivariate adaptive regression splines and neural network models for prediction of pile drivability. *Geosci Front* 7:45–52. <https://doi.org/10.1016/j.gsf.2014.10.003>
- Zhou Y, Guo S, Chang F-J (2019) Explore an evolutionary recurrent ANFIS for modelling multi-step-ahead flood forecasts. *J Hydrol* 570:343–355. <https://doi.org/10.1016/j.jhydrol.2018.12.040>

**Publisher's Note** Springer Nature remains neutral with regard to jurisdictional claims in published maps and institutional affiliations.

## Affiliations

Zaher Mundher Yaseen<sup>1</sup> · Sujay Raghavendra Naganna<sup>2</sup> · Zulfaqar Sa'adi<sup>3</sup> · Pijush Samui<sup>4</sup> · Mohammad Ali Ghorbani<sup>5,6</sup> · Sinan Q. Salih<sup>7,8</sup> · Shamsuddin Shahid<sup>9</sup>

<sup>1</sup> Sustainable Developments in Civil Engineering Research Group, Faculty of Civil Engineering, Ton Duc Thang University, Ho Chi Minh City, Vietnam

<sup>2</sup> Department of Civil Engineering, Shri Madhwa Vadiraja Institute of Technology and Management, Bantakal-574115, Udipi, India

<sup>3</sup> Center for environmental and sustainability and water security (IPASA), School of Civil Engineering, Faculty of Engineering, Universiti Teknologi Malaysia, 81310 Skudai, Johor Bahru, Malaysia

<sup>4</sup> Department of Civil Engineering, National Institute of Technology Patna, Bihar, India

<sup>5</sup> Department of Water Engineering, University of Tabriz, Tabriz, Iran

<sup>6</sup> Department of Civil Engineering, Near East University, P.O. Box: 99138, Nicosia, North Cyprus, Mersin, Turkey

<sup>7</sup> Institute of Research and Development, Duy Tan University, Da Nang 550000, Vietnam

<sup>8</sup> Computer Science Department, College of Computer Science and Information Technology, University of Anbar, Ramadi, Iraq

<sup>9</sup> School of Civil Engineering, Faculty of Engineering, Universiti Teknologi Malaysia, 81310 Skudai, Johor Bahru, Malaysia